Journal of Alloys and Compounds 506 (2010) 338–342

Contents lists available at ScienceDirect

Journal of Alloys and Compounds

journal homepage: www.elsevier.com/locate/jallcom

Thermal stable $La_2Ti_2O_7:Eu^{3+}$ phosphors for blue-chip white LEDs with high color rendering index

Zhuang Sun [a], Qinghong Zhang [a], Yaogang Li [b], Hongzhi Wang [a,*]

[a] State Key Laboratory for Modification of Chemical Fibers and Polymer Materials, Donghua University, 2999 North Renming Road, Songjiang, Shanghai 201620, China
[b] Engineering Research Center of Advanced Glasses Manufacturing Technology, MOE, Donghua University, Shanghai 201620, China

ARTICLE INFO

Article history:
Received 17 February 2010
Received in revised form 17 June 2010
Accepted 22 June 2010
Available online 13 July 2010

Keywords:
Phosphors
Solid state reactions
Eu-doped
$La_2Ti_2O_7$
Luminescence

ABSTRACT

High concentration Eu^{3+} doped $La_2Ti_2O_7$ phosphor with good crystallinity was prepared via solid-state method. This phosphor can emit intense red light with a peak around 612 nm corresponding to the $^5D_0 \rightarrow {}^7F_2$ transitions of Eu^{3+}. The luminescent intensity excited at 465 nm, which corresponds to the wavelength of InGaN-based LEDs, is comparable with the intensity excited at 396 nm. The emission intensity increased with increasing Eu^{3+} concentration up to 30 mol%, and then decreased due to the concentration quenching. The White LED (WLED) fabricated by coating a mixture of $Y_3Al_5O_{12}:Ce^{3+}$ and $La_2Ti_2O_7:Eu^{3+}$ onto a blue InGaN chip showed higher color rendering index than the WLED fabricated by coating $Y_3Al_5O_{12}:Ce^{3+}$($Y_3Al_5O_{12}:Ce^{3+}$-WLED). This phosphor also has excellent thermal stability, and the luminous intensity can remain 75.46% when it was heated to 200°. By optimizing the Eu^{3+} concentration and calcination temperature, we demonstrated that $La_2Ti_2O_7:Eu^{3+}$ was a promising red phosphor under blue light (465 nm) for high-power commercial $Y_3Al_5O_{12}:Ce^{3+}$-WLEDs.

1. Introduction

Compared with the traditional lighting engineering (incandescent, fluorescent lamps), semiconductor white LED lighting is considered as a novel generation of light source [1,2]. With the development of semiconductor technology, much progress has been made in the art of high-brightness LEDs with various colors. Especially, the invention of the blue LED based on GaN was regarded as a triumph of material chemistry. For the first time it is possible to generate white light from LEDs equaling halogen lamps in efficiency [3,4].

A device has been commendably realized by coating $Y_3Al_5O_{12}:Ce^{3+}$ yellow phosphor on the blue LED chip. However, this device has a rather low color render index, viz., the output light is deficient in the red region of the sunlight spectrum (above 600 nm) [5]. Currently, $Y_2O_2S:Eu^{3+}$ [6] is used as the commercially applicable red phosphor, however, it is chemically unstable in atmosphere and has low efficiency. At present, a great deal of research is being carried out to find a desirable red-emitting phosphor for white LEDs. Zhou et al. [7] synthesized a series of red phosphors $La_{1-x}Nb_{0.70}V_{0.30}O_4:Eu^{3+}{}_x$ and measured their photoluminescent properties for white light-emitting diodes. Fu et al. [8,9] investigated the luminescent properties of $Ca_{1-x}TiO_3:Eu^{3+}{}_x$ red-emitting phosphors for LEDs. Xie et al. [10] obtained $Na_{0.5-y}Li_yGd_{0.5-x}MoO_4:Eu^{3+}{}_x$ phosphors and investigated their luminescence in detail. However, $La_{1-x}Nb_{0.70}V_{0.30}O_4:Eu^{3+}{}_x$, $Ca_{1-x}TiO_3:Eu^{3+}{}_x$ and $Na_{0.5-y}Li_yGd_{0.5-x}MoO_4:Eu^{3+}{}_x$ phosphors were all doped by Eu^{3+} with a high concentration, e.g. $La_{1-x}Nb_{0.70}V_{0.30}O_4:Eu^{3+}{}_x$ ($x = 30\%$), $Ca_{1-x}TiO_3:Eu^{3+}{}_x$ ($x = 28\%$) and $Na_{0.5-y}Li_yGd_{0.5-x}MoO_4:Eu^{3+}{}_x$ ($x = 50\%$), but the reason for the high concentration quenching of Eu^{3+} ions in these matrices were not discussed in detail and they were mainly investigated for the NUV LED chips, there are very few reports about red phosphors for the $Y_3Al_5O_{12}:Ce^{3+}$-WLEDs. Furthermore, the thermal stability problem caused by the heat generated within the LEDs themselves is still a bottleneck to limit the reliability and lifetime of high-power LEDs [11]. So, a novel red-light phosphor, which has good thermal stability, high color rendering index and good wavelength matching with most commercial LED Chips, has to be developed.

Because of high Curie temperature and excellent piezoelectric and electrooptic properties, $La_2Ti_2O_7$ has been studied as electrical and optical device [12,13]. The monoclinic structure of $La_2Ti_2O_7$ has layered perovskite structure and different distance of donor–donor in different directions for the lanthanide ions, which offers the possibility of high concentration ions-doped. Furthermore, $La_2Ti_2O_7$ can act as excellent hosts/matrices for rare earth ions to produce phosphors emitting a variety of colors [14–16]. However, in the reports about $(La, Pr)_2Ti_2O_7$ [14] and $(La_{0.95-x}Eu_{0.05}Li_x)_2Ti_2O_7$ [16], the excitation spectrums mainly locate at 337 and 286 nm, respectively, which are not applicable to LED chips.

In this paper, we report that a thermal stable red phosphor with high concentration of Eu molar percentages up to 30 has

* Corresponding author.
E-mail address: wanghz@dhu.edu.cn (H. Wang).

0925-8388/$ – see front matter © 2010 Elsevier B.V. All rights reserved.
doi:10.1016/j.jallcom.2010.06.203

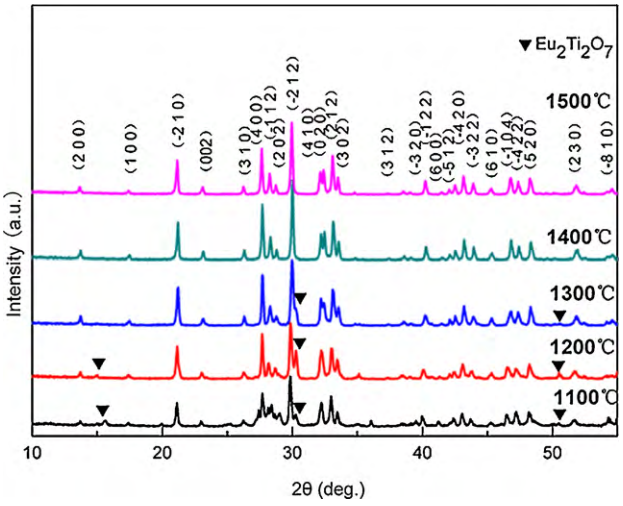

Fig. 1. XRD spectra of $La_2Ti_2O_7:Eu^{3+}$ (30 mol%) calcined at different temperatures.

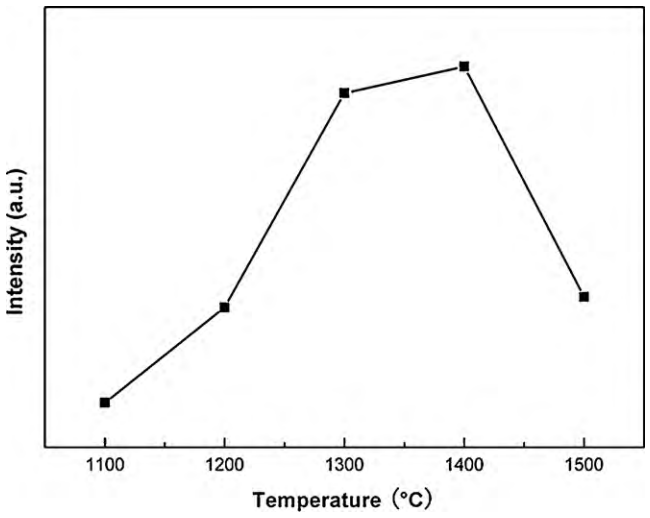

Fig. 2. Effect of temperature on the PL intensity of $La_2Ti_2O_7:Eu^{3+}$ (30 mol%).

been obtained. The WLED fabricated by coating a mixture of $Y_3Al_5O_{12}:Ce^{3+}$ and $La_2Ti_2O_7:Eu^{3+}$ onto blue InGaN chip showed higher color rendering index than the $Y_3Al_5O_{12}:Ce^{3+}$-WLED. Furthermore, when the temperature was increased to 200°, the luminous intensity of this phosphor remained 75.46% compared with that at room temperature. So, this phosphor was a promising red phosphor for high-power commercial $Y_3Al_5O_{12}:Ce^{3+}$-WLEDs.

2. Experimental

2.1. Synthesis of $La_2Ti_2O_7:Eu^{3+}$ phosphors

Europium-doped lanthanum titanate powder was prepared by a solid-state reaction route. Starting powders weighed out from La_2O_3 (Analytical reagent, China National Medicines Co. Ltd.), TiO_2 (Analytical reagent, China National Medicines Co. Ltd.), and Eu_2O_3 (Analytical reagent, China National Medicines Co. Ltd.) were well mixed in a mortar. The concentration of the dopant varied in a range of 6–35 mol% with respect to Eu. The powder mixture was packed into an alumina crucible and fired in a muffle furnace. The samples were heated at a constant heating rate of 400 °C/h from room temperature to a high temperature in a range of 1100–1500 °C for 2 h. The fired powder samples were nearly phase pure, analyzed by the X-ray diffraction technique. In addition, the sample $Y_3Al_5O_{12}:Ce^{3+}$ (Analytical reagent, China, Jiangsu Bree Optronics Co., Ltd) was bought from company, which has been widely used in the LEDs production.

2.2. Characterization

The powder phase compositions were identified by a X-ray diffractometer (Model D/MAX-2550, Rigaku, Japan) using Cu Kα radiation (λ=1.5406 Å) at 40 kV and 100 mA. For the photoluminescent (PL) analysis, both the excitation and the emission spectra of the phosphors were measured using a fluorescence spectrophotometer (Model FP-6600, JASCO, Japan). The color rendering index and CIE chromaticity coordinates were measured by an optoelectronics system (Model HSP-3000, Hongpu, China) under 20 mA.

3. Results and discussion

3.1. Effects of calcination temperatures and doping concentrations

The crystallinity of the materials was systematically checked by XRD as shown in Fig. 1. The diffraction patterns of the samples calcinated from 1100 °C to 1300 °C showed that there were still some impurities, i.e., a cubic $Eu_2Ti_2O_7$ structure. When the samples were calcinated above 1400 °C, all the peaks were attributed to the $La_2Ti_2O_7$ phase (JCPDS file 28-0517), revealing that Eu ions were effectively doped into the host lattice. The strongest peak of the $La_2Ti_2O_7:Eu^{3+}$ structure was centered at $2\theta = 29.81°$ and corresponded to the crystalline plane with Miller indices of (−2 1 2).

Fig. 2 shows the PL intensities of the $La_2Ti_2O_7:Eu^{3+}$ powders after calcination at 1100 °C, 1200 °C, 1300 °C, 1400 °C and 1500 °C, respectively. The emission intensities of the samples increased with the elevated calcination temperatures under the excitation of 465 nm. The strongest emission intensity was observed from the sample calcinated at 1400 °C, which was due to the better crystallinity. However, the intensity sharply decreased when this sample was calcinated at 1500 °C. The possible reason is that some defects were generated in the sample at 1500 °C.

The emission intensities of $La_2Ti_2O_7:Eu^{3+}$ particles with different doping concentrations of Eu were shown in Fig. 3. The optimal concentration for obtaining the strongest PL intensity of $La_2Ti_2O_7:Eu^{3+}$ was 30 mol% of Eu (calcinated at 1400 °C for 2 h), then decreased due to the concentration quenching. Such high concentration was due to the layered perovskite structure and different distance of Eu^{3+}–Eu^{3+} in different directions in $La_2Ti_2O_7$ matrices.

3.2. The structure and high concentration of $La_2Ti_2O_7:Eu^{3+}$

From JCPDS file 28-0517, we can find the $La_2Ti_2O_7$ structure belongs to the monoclinic system with the space group $P2_1$ and the unit cell parameters $a = 5.546$ Å, $b = 7.817$ Å, $c = 13.015$ Å and

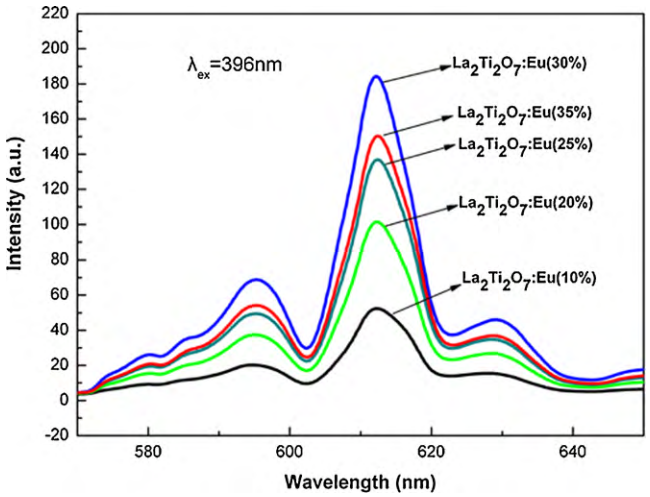

Fig. 3. Emission spectra of $La_2Ti_2O_7:Eu^{3+}$ calcined at 1400 °C with different Eu-doped concentration.

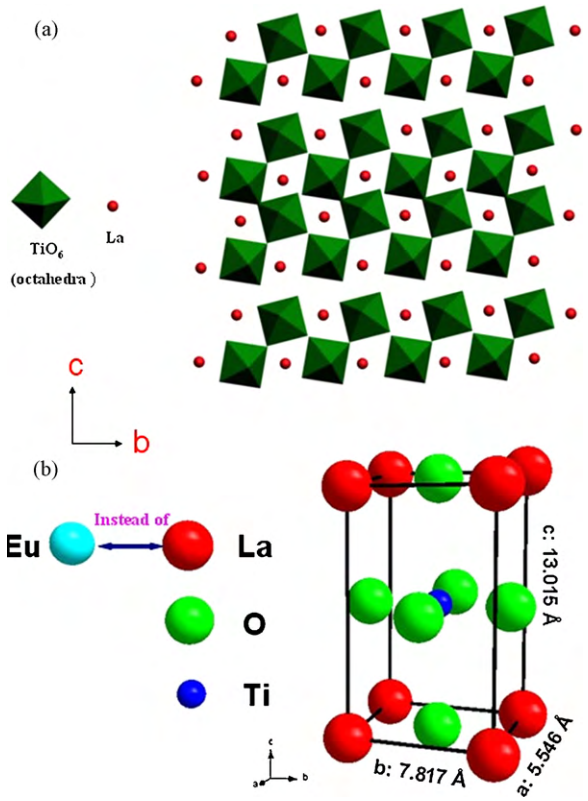

Fig. 4. (a) Projections of $La_2Ti_2O_7$ structure on the bc plane and (b) simulated monoclinic lattice of the $La_2Ti_2O_7$:Eu^{3+} samples in the layers.

$\gamma = 98.64^\circ$. For the solid solution $La_2Ti_2O_7$:Eu^{3+}, the structure was confirmed with Eu molar percentages up to 30%. The crystal structure of $La_2Ti_2O_7$ is built up of layers of distorted perovskite-likes slabs, which run parallel to the (1 0 0) plane and are bounded to each other by interlayer La^{3+} ions as showed in Fig. 4a. The thickness of the slabs corresponds approximately to four corner-linked TiO_6 octahedra [15,17].

In the $La_2Ti_2O_7$:Eu^{3+}, the high concentration quenching might be due to the restrain of energy transfer between the Eu ions because of the large energy transfer distance. The critical concentration of an activator in a given host lattice provides a direct measure of R_C, which is the shortest distance between nearest activator ions and can be found from [18]:

$$R_C \approx 2 \times \left(\frac{3V}{4\pi X_c N}\right)^{1/3}$$

Here X_c is the critical concentration, N is the number of Z ions in the unit cell if the activator is introduced solely on Z ion sites, and V is the volume of the unit cell. According to our understanding, V is 557.8 for $La_2Ti_2O_7$, X_c is 0.3, N is 1 for La^{3+} in the $La_2Ti_2O_7$ structure, therefore, the critical distance R_C for energy transfer between the Eu ions in the $La_2Ti_2O_7$:Eu^{3+} (30 mol%) was calculated as 15.26 Å. From the Blasse's theory [19], if the Eu^{3+}–Eu^{3+} distance is larger than 5 Å, exchange interaction becomes ineffective. Only multipolar interactions are of importance, and they will be weak anyhow. Actually, if sufficiently pure, $EuAl_3B_4O_{12}$ (Eu–Eu 5.9 Å), $Eu(IO_3)_3$ (Eu–Eu 5.9 Å) and $CsEuW_2O_8$ (Eu–Eu 5.2 Å) luminesce efficiently at 300 K. In this case, 15.26 > 5 Å, the average distance between the Eu ions is so large that the migration is hampered and the killers are not reached, which makes the high concentration quenching possible in the $La_2Ti_2O_7$:Eu^{3+}.

Furthermore, another possible reason for the high concentration quenching may be due to the regular energy transfer in this

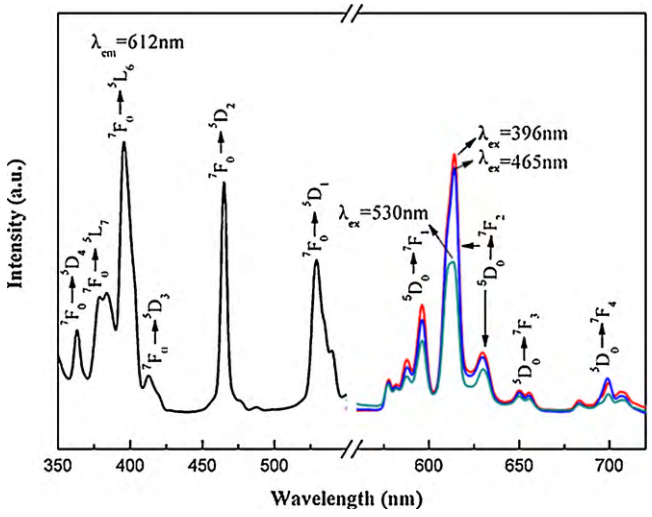

Fig. 5. Emission and excitation spectra of $La_2Ti_2O_7$:Eu^{3+} (20 mol%, 1400 °C).

structure. It is assumed that the donor–donor energy transfer in the interlayer is restricted because the distance of interlayer Eu^{3+} ions is larger than the Eu^{3+} ions in the layers from Fig. 4a. Meanwhile, the energy transfer in the layers' region is alternative because of the energy transfer distance between Eu^{3+} ions along the "*a*" ($R_a \approx 10.28$ Å) axis are smaller than the distance between Eu^{3+} ions along "*b*" ($R_b \approx 14.49$ Å) or "*c*" ($R_c \approx 24.13$ Å) axis, which makes the possibility for the energy transfer on the "*b*" or "*c*" axis much lower. This can also be verified by the $La_2Ti_2O_7$ structure's characteristic as shown in Fig. 4b, the distance between La^{3+} ions along the "*a*" axis (5.546 Å) are smaller than the distance between La^{3+} ions along "*b*" (7.817 Å) or "*c*" (13.015 Å) axis. So, the Eu^{3+}–Eu^{3+} energy transfer in this structure is regular, which is not chaotic and random like in other hosts. Therefore, the high concentration quenching of Eu^{3+} ions may occur in this matrix.

3.3. Emission and excitation spectra

Fig. 5 (left) shows the excitation spectra of $La_2Ti_2O_7$:Eu^{3+}. It can be seen clearly that the excitation spectrum mainly exists at about 396, 465 and 530 nm, and the highest peak was 396 nm. It is worth noting that the peak of 465 nm was comparable with the 396 nm, much higher than the 530 nm. The f–f transitions within the Eu^{3+} are in the long spectral region with $^7F_0 \rightarrow {}^5D_4$ (363 nm), $^7F_0 \rightarrow {}^5L_7$ (381 nm), $^7F_0 \rightarrow {}^5D_3$ (413 nm), $^7F_0 \rightarrow {}^5L_6$ (396 nm), $^7F_0 \rightarrow {}^5D_2$ (465 nm) [20] and $^7F_0 \rightarrow {}^5D_1$ (530 nm) as the most prominent group.

The emission spectrum of $La_2Ti_2O_7$:Eu^{3+} (Fig. 5, right) exhibits five obvious maximum allocated at 580, 595, 612, 652 and 701 nm, being assigned to transitions from the excited ^5D_o state to ^7F_J (J = 0–4) levels of the Eu^{3+} [8,21], respectively. The most intense band at 612 nm is due to the $^5D_0 \rightarrow {}^7F_2$ transition and the intensity excited at 465 nm is comparable to the 396 nm, much higher than the 530 nm, which is corresponding with the Fig. 5, left. The $^5D_0 \rightarrow {}^7F_1$ band at 595 nm is a magnetic dipole one and hardly varies with the crystal field strength around the Eu^{3+}, but the electric dipole transition $^5D_0 \rightarrow {}^7F_2$ is very sensitive to the local environment around the Eu^{3+}, and its intensity depends on the symmetry of the crystal field around the Eu^{3+} [9,22]. The asymmetry ratio ($^5D_0 \rightarrow {}^7F_2$)/($^5D_0 \rightarrow {}^7F_1$) of the $La_2Ti_2O_7$:Eu^{3+} (20%) is calculated as 2.56, indicating that the Eu^{3+} ions occupy low-symmetry sites. It is assumed that this phosphor can be used in conjunction with the InGaN-chip to emit red light, which can

Table 1
The performance parameters of the LEDs.

LED	Excitation wavelength (nm)	Excitation electric current (mA)	CIE chromaticity coordinates		Color rendering index
			x	*y*	
WLED made from $Y_3Al_5O_{12}:Ce^{3+}$ and a blue InGaN Chip	465	20	0.3259	0.3487	77.9
WLED made from $Y_3Al_5O_{12}:Ce^{3+}$, $La_2Ti_2O_7:Eu^{3+}$ and a blue InGaN Chip	465	20	0.2809	0.2737	84.9

resolve the problem of undesirable color balance for the true color rendition.

3.4. Fabricated LED

Fig. 6 shows the emission spectra of $La_2Ti_2O_7:Eu^{3+}$ and $La_2Ti_2O_7:Eu^{3+}$ and $Y_3Al_5O_{12}:Ce^{3+}$ exited at 465 nm. In the spectra of $La_2Ti_2O_7:Eu^{3+}$ and $Y_3Al_5O_{12}:Ce^{3+}$, there are two main peaks, 541 and 612 nm, which come from $Y_3Al_5O_{12}:Ce^{3+}$ and $La_2Ti_2O_7:Eu^{3+}$, respectively. Furthermore, the 612 nm intensity of mixture phosphors is much higher than the $La_2Ti_2O_7:Eu^{3+}$, the possible reason is that the $La_2Ti_2O_7:Eu^{3+}$ can also be excited from the wavelength band from 520 to 546 nm (Fig. 5, left) and emit red light. Therefore, when the mixture phosphors were excited by 465 nm, the $La_2Ti_2O_7:Eu^{3+}$can emit red light, meanwhile, the $La_2Ti_2O_7:Eu^{3+}$ can be also excited by the emission wavelength coming from $Y_3Al_5O_{12}:Ce^{3+}$. This property is advantageous to obtain good CIE chromaticity coordinates for the phosphors. The WLEDs were fabricated with $Y_3Al_5O_{12}:Ce^{3+}$ and a mixture of $Y_3Al_5O_{12}:Ce^{3+}$ and $La_2Ti_2O_7:Eu^{3+}$ onto blue InGaN chips. Both WLEDs exhibited bright white emitting and the CIE chromaticity coordinates are (0.3259, 0.3487) for the $Y_3Al_5O_{12}:Ce^{3+}$-WLED and (0.2809, 0.2737) for the mixture-WLED, respectively (Table 1). Therefore, the CIE coordinates for the mixture-WLED showed red shift compared with that for the $Y_3Al_5O_{12}:Ce^{3+}$-WLED. With the red light of $La_2Ti_2O_7:Eu^{3+}$, the color rendering index for the mixture-WLED phosphor (84.9) is higher than the $Y_3Al_5O_{12}:Ce^{3+}$-WLED (77.9), the performance of the mixture-WLED was improved on the CIE coordinates and color rendering index. The results indicate that the phosphor can be a promising red component for the commercial $Y_3Al_5O_{12}:Ce^{3+}$-WLEDs.

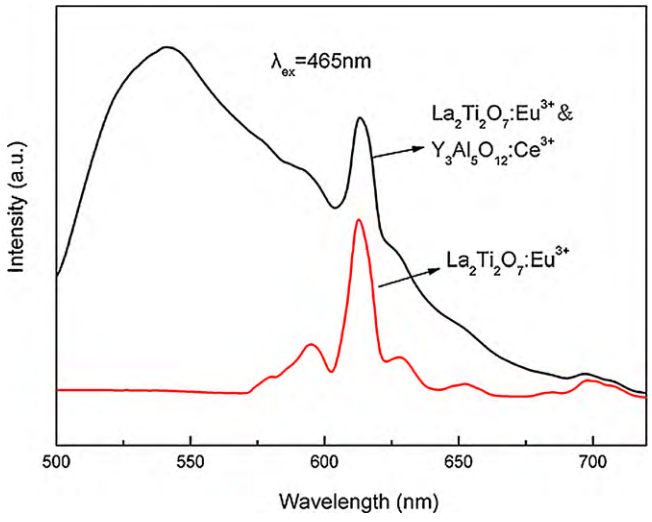

Fig. 6. Emission spectra of $La_2Ti_2O_7:Eu^{3+}$ and $La_2Ti_2O_7:Eu^{3+}$ and $Y_3Al_5O_{12}:Ce^{3+}$ excited at 465 nm.

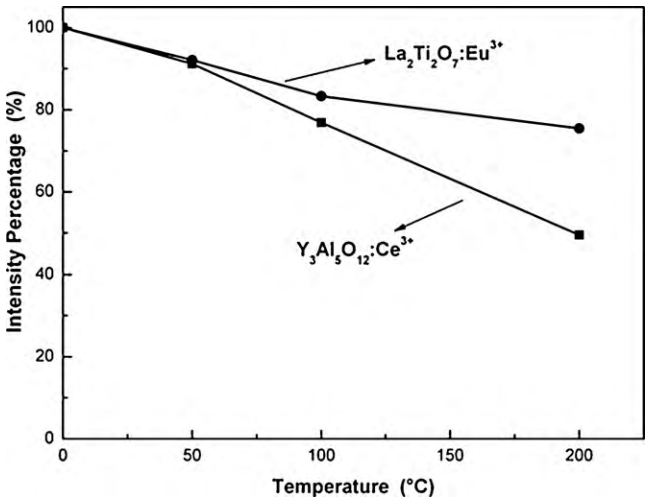

Fig. 7. The luminous intensities of $La_2Ti_2O_7:Eu^{3+}$ and $Y_3Al_5O_{12}:Ce^{3+}$ with raised temperatures.

3.5. Thermal stability

$La_2Ti_2O_7:Eu^{3+}$ also has very good thermal stability. Fig. 7 shows the luminous intensity changes of $La_2Ti_2O_7:Eu^{3+}$ and $Y_3Al_5O_{12}:Ce^{3+}$ with raised temperatures. We can see that the thermal stabilities were similar to each other when the temperature was less than 100°. But when the temperature was increased to 150°, the luminous intensity of $Y_3Al_5O_{12}:Ce^{3+}$ dropped to 76.89% while $La_2Ti_2O_7:Eu^{3+}$ dropped to 83.28%. When the temperature was increased to 200°, the luminous intensity of $Y_3Al_5O_{12}:Ce^{3+}$ remained only 49.51% while $La_2Ti_2O_7:Eu^{3+}$ remained 75.46%. The good thermal stability of $La_2Ti_2O_7:Eu^{3+}$ can be attributed to its special structure. viz., the layered perovskite structure. Because of this performance, this phosphor can replace the unstable alkaline-earth sulfides to emit red light and meet the demand of high-power LEDs.

4. Conclusions

In this work, $La_2Ti_2O_7:Eu^{3+}$ phosphors were synthesized by a solid state reaction method, which have good thermal stability and strong luminescent intensity. XRD spectra showed a well-defined crystalline structure without impurity phases for doped samples. The crystalline $La_2Ti_2O_7:Eu^{3+}$ phosphors showed emission peaks from 575 to 720 nm and the maximum emission wavelength was at 612 nm. Because this phosphor was efficiently excited by 465 nm, it can well match the blue LED Chips. The WLED fabricated by coating a mixture of $Y_3Al_5O_{12}:Ce^{3+}$ and $La_2Ti_2O_7:Eu^{3+}$ onto blue InGaN chip showed higher color rendering index than the $Y_3Al_5O_{12}:Ce^{3+}$-WLED and its good thermal stability can meet the demand of high-power LEDs. The emission intensity increased steadily with the increasing of the calcination temperature till 1500 °C. The optimized Eu doping concentration was found to be 30 mol% for the

emission intensity reached the top. The phosphor obtained by our experiments could find extensive applications in high-power commercial $Y_3Al_5O_{12}:Ce^{3+}$-WLEDs.

Acknowledgments

We gratefully acknowledge the financial supports by Shanghai Municipal Education Commission (No. 07SG37), National Natural Science Foundation of China (No. 50772022, 50772127), Shanghai Leading Academic Discipline Project (B603), the Cultivation Fund of the Key Scientific and Technical Innovation Project (No. 708039), and the Program of Introducing Talents of Discipline to Universities (No. 111-2-04).

References

[1] X.Y. Sun, J.H. Zhang, X. Zhang, S.Z. Lu, X.J. Wang, J. Lumin. 122 (2007) 955–957.
[2] L.Y. Zhou, J.L. Huang, L.H. Yi, M.L. Gong, J.X. Shi, J. Rare Earths 27 (2009) 54–57.
[3] R. Mueller-Mach, G.O. Mueller, M.R. Krames, J. IEEE 8 (2002) 339–345.
[4] C.R. Ronda, T. Justel, H. Nikol, J. Alloys Compd. 275–277 (1998) 669–676.
[5] Y.S. Hu, W.D. Zhuang, H.Q. Ye, S.S. Zhang, Y. Fang, X.W. Huang, J. Lumin. 111 (2005) 139–145.
[6] S. Neeraj, N. Kijima, A.K. Cheetham, Chem. Phys. Lett. 387 (2004) 2–6.
[7] L.Y. Zhou, J.L. Huang, F.Z. Gong, Y.W. Yu, Z.F. Tong, J.H. Sun, J. Alloys Compd. 495 (2010) 268–271.
[8] J.P. Fu, Q.H. Zhang, Y.G. Li, H.Z. Wang, J. Alloys Compd. 485 (2009) 418–421.
[9] J.P. Fu, Q.H. Zhang, Y.G. Li, H.Z. Wang, J. Lumin. 130 (2010) 231–235.
[10] A. Xie, X.M. Yuan, F.X. Wang, Y. Shi, J. Alloys Compd. 501 (2010) 124–129.
[11] X.Y. Lu, T.C. Hua, M.J. Liu, Y.X. Cheng, Thermochim. Acta 493 (2009) 25–29.
[12] Y.A. Titov, A.M. Sych, V.Y. Markiv, N.M. Belyavina, A.A. Kapshuk, V.P. Yaschuk, J. Alloys Compd. 316 (2001) 309–315.
[13] A.D. Li, Y.J. Wang, S. Huang, J.B. Cheng, D. Wu, N.B. Ming, J. Cryst. Growth 268 (2004) 198–203.
[14] P.T. Diallo, P. Boutinaud, R. Mahiou, J.C. Cousseins, J. Alloys Compd. 275–277 (1998) 307–310.
[15] P.T. Diallo, P. Boutinaud, R. Mahiou, J. Alloys Compd. 341 (2002) 139–143.
[16] H.H. Yang, H. Cheng, Y.G. Tang, Z.G. Lu, Am. Ceram. Soc. 92 (2009) 931–933.
[17] M. Gasperin, Acta Cryst. B31 (1975) 2129–2130.
[18] G. Blasse, Philps Res. Rep. 24 (1969) 131–144.
[19] G. Blass, B.C. Grabmaier, Luminescent Materials, Springer-Verlag, Berlin, Heidelberg, 1994, p. 99.
[20] I. Omkaram, B. Vengala Rao, S. Buddhudu, J. Alloys Compd. 474 (2009) 565–568.
[21] B. Vengala Rao, U. Rambabu, S. Buddhudu, Phys. B 382 (2006) 86–91.
[22] M. Nogami, T. Enomoto, T. Hayakawa, J. Lumin. 97 (2002) 147–152.